Acta Astronautica 123 (2016) 229–238

Contents lists available at ScienceDirect

Acta Astronautica

journal homepage: www.elsevier.com/locate/aa

Aerodynamic analysis of the aerospaceplane HyPlane in supersonic rarefied flow

Gennaro Zuppardi [a,*], Raffaele Savino [a], Gennaro Russo [b,c], Luca Spano' Cuomo [a], Eliano Petrosino [a]

[a] Department of Industrial Engineering, Aerospace Division, University of Naples "Federico II", Piazzale Tecchio 80, 80125 Naples, Italy
[b] Trans-Tech Srl, Via Palizzi 107, 80127 Naples, Italy
[c] Near Space of the Italian Institute for the Future, Via Guido de Ruggiero 52, 80128 Naples, Italy

ARTICLE INFO

Article history:
Received 13 November 2015
Received in revised form
4 March 2016
Accepted 24 March 2016
Available online 28 March 2016

Keywords:
Aerospaceplane aerodynamics
Supersonic flow
Aerodynamic surface attitude control
Rarefied gas dynamics
Direct Simulation Monte Carlo method

ABSTRACT

HyPlane is the Italian aerospaceplane proposal targeting, at the same time, both the space tourism and point-to-point intercontinental hypersonic flights. Unlike other aerospaceplane projects, relying on boosters or mother airplanes that bring the vehicle to high altitude, HyPlane will take off and land horizontally from common runways. According to the current project, HyPlane will fly sub-orbital trajectories under high-supersonic/low-hypersonic continuum flow regimes. It can go beyond the von Karman line at 100 km altitude for a short time, then starting the descending leg of the trajectory. Its aerodynamic behavior up to 70 km have already been studied and the results published in previous works. In the present paper some aspects of the aerodynamic behavior of HyPlane have been analyzed at 80, 90 and 100 km. Computer tests, calculating the aerodynamic parameters, have been carried out by a Direct Simulation Monte Carlo code. The effects of the Knudsen, Mach and Reynolds numbers have been evaluated in clean configuration. The effects of the aerodynamic surfaces on the rolling, pitching and yawing moments, and therefore on the capability to control attitude, have been analyzed at 100 km altitude. The aerodynamic behavior has been compared also with that of another aerospaceplane at 100 km both in clean and flapped configuration.

1. Introduction

HyPlane [1–4] is a small, six seats, hypersonic aerospaceplane. Its dimensions are similar to those of a business jet and, just like an usual airplane, it is able to perform Horizontal Take-off and Horizontal Landing (HTHL) on common runways. For this reason, according to the logic "a closer space and aeronautics" [5], this vehicle can be considered as the "natural" transition of the space vehicles concept toward the future civil aviation or toward the development of trans-atmospheric, totally re-usable vehicle. In other words, it moves toward much lower costs than other aerospaceplane concepts relying on boosters, as per Space Shuttle [6] and SpaceLiner [7–9], or mother ship carrier as per SpaceShipTwo [10].

Architecture of HyPlane is similar to that of Concorde [11] but its dimensions are much smaller; the linear dimensions are reduced of about 50%. HyPlane is powered by Turbine Based Combined Cycle (TBCC) turbo-ramjet engines plus a throtteable rocket, consuming less fuel than that of the engine of the Blackbird SR-71 Lockheed aircraft. Current studies are based on the use of advanced and green fuels (JP7, JP10, biofuel).

HyPlane has been designed to fly in stratosphere (at 30 km altitude) and at cruising speed of about 5000 km/h (Mach number about 4.6), covering distances like Rome–New York in less than 2 h. Turbojet mode will be used for take-off and for reaching supersonic velocity, while ramjet mode will allow reaching hypersonic velocity at high altitude. HyPlane has been also designed as a space tourism vehicle; thanks to the boosting function of the rocket motor, it can reach altitudes of at least 70 km twice or three times per flight in order to provide the passengers with an amazing view of Earth while they are floating in low gravity. Fig. 1 (a) and (b) show rendering of HyPlane aeroshape and of the passengers cabin respectively. Three large portholes on the top of the passengers cabin are indicative of its tourism vocation.

It is well known that the success of the aerodynamic design of an aerospaceplane is linked to its capability of controlling attitude and restoring equilibrium in rarefied flow. These functions, for all space vehicles, are undertaken by thrusters. Controlling attitude also by means of aerodynamic surfaces simplifies this task. In addition, an aerospaceplane should carry a lower amount of fuel

* Corresponding author.
E-mail address: zuppardi@unina.it (G. Zuppardi).

http://dx.doi.org/10.1016/j.actaastro.2016.03.025
0094-5765/

List of symbols

b	wing span
C_D, C_L	drag, lift coefficients
C_{Mx}, C_{My}, C_{Mz}	rolling, yawing, pitching (or longitudinal) moment coefficients
C_p	pressure coefficient
c_p	constant pressure specific heat
$\bar{d}$	average diameter of the colliding molecules
f	fraction of molecules diffusively re-emitted
H	specific total enthalpy ($H=V^2/2+c_pT$)
h	altitude
Kn	Knudsen number (Kn$=\lambda/L$)
L	length
L_x, L_y, L_z	dimensions of computing region along the x-, y-and z-axis
M	Mach number ($M = V/\sqrt{\gamma RT}$)
M_x, M_y, M_z	rolling, yawing, pitching (or longitudinal) moments
mcs	mean collision separation
N	number density
p_D	dynamic pressure ($p_D=1/2\rho V^2$)
R	gas constant
Re	Reynolds number (Re$=\rho VL/\mu$)
S	surface
T	temperature
t_s	simulation time
t_f	time to travel the computing region at the free stream velocity
V	velocity

Greek symbols

α	angle of attack
$^{\alpha}O_2$, α_{N_2}, α_O	molar fraction of oxygen, nitrogen and atomic oxygen
γ	rudder deflection or ratio constant pressure specific heat on constant volume specific heat
Δ	finite difference
δ	flap deflection
λ	free molecule path ($\lambda = 1/(\sqrt{2}\pi\bar{d}^2N)$
μ	viscosity
ϑ	aileron deflection
ρ	density

Subscripts

i	incompressible
ref	reference
w	wing or wall
∞	free stream

Acronyms

CoM	Center of Mass
DSMC	Direct Simulation Monte Carlo

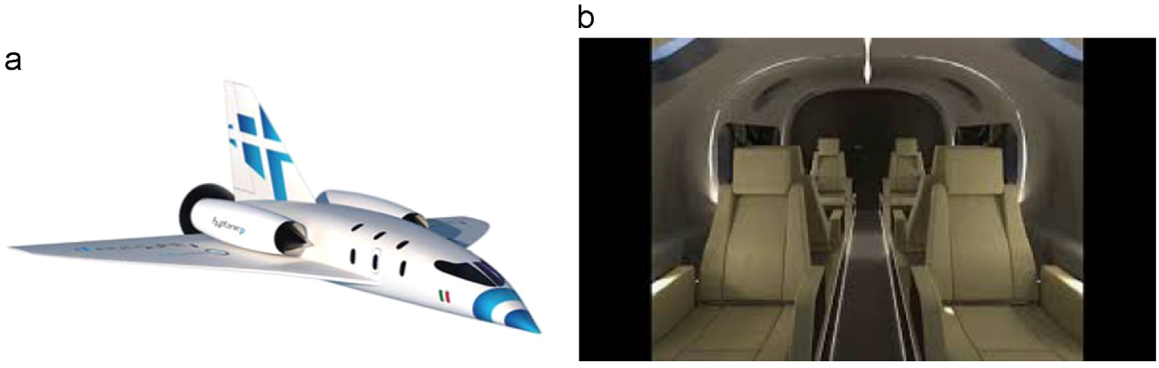

Fig. 1. (a) Rendering of HyPlane, and (b) interior view of the passengers cabin.

for the thrusters. This issue is important and deserves to be studied with the aim of providing the aerospaceplane designer with useful information about the aerodynamic control of the vehicle.

Aerodynamics of HyPlane in the continuum regime and the flow field local phenomena at the altitudes where they are mostly relevant have been already studied [2]. The aim of this paper is twofold:

1) Studying the global aerodynamic behavior of HyPlane in high altitude supersonic, rarefied flow field and at two Mach numbers (2 and 3), representing the estimated maximum speeds at the apex of sub-orbital trajectories up to 100 km altitude. The aerodynamic computations have been carried out by the Direct Simulation Monte Carlo code DS3V [12] at the altitudes of 80, 90 and 100 km. The aerodynamic behavior has been compared also with that of SpaceLiner [9] at 100 km both in clean and flapped configuration.
2) Evaluating the effectiveness of the HyPlane aerodynamic control surfaces (flaps, ailerons and rudder). The analysis has been carried out at 100 km altitude and at zero angle of attack, evaluating the influence on the pitching (or longitudinal), rolling and yawing moments of the control aerodynamic surfaces.

2. HyPlane configuration

Fig. 2(a), (b) and (c) show the top, the lateral and the front views of HyPlane, respectively. All linear dimensions are in meters. The net and the gross weights of HyPlane are about 9.2×10^3 and 2.7×10^4 kg, respectively. Considering the origin of the reference system located in the tip of the airplane nose, the x (roll) axis is along the fuselage from nose to tail, the y (yaw) axis is from

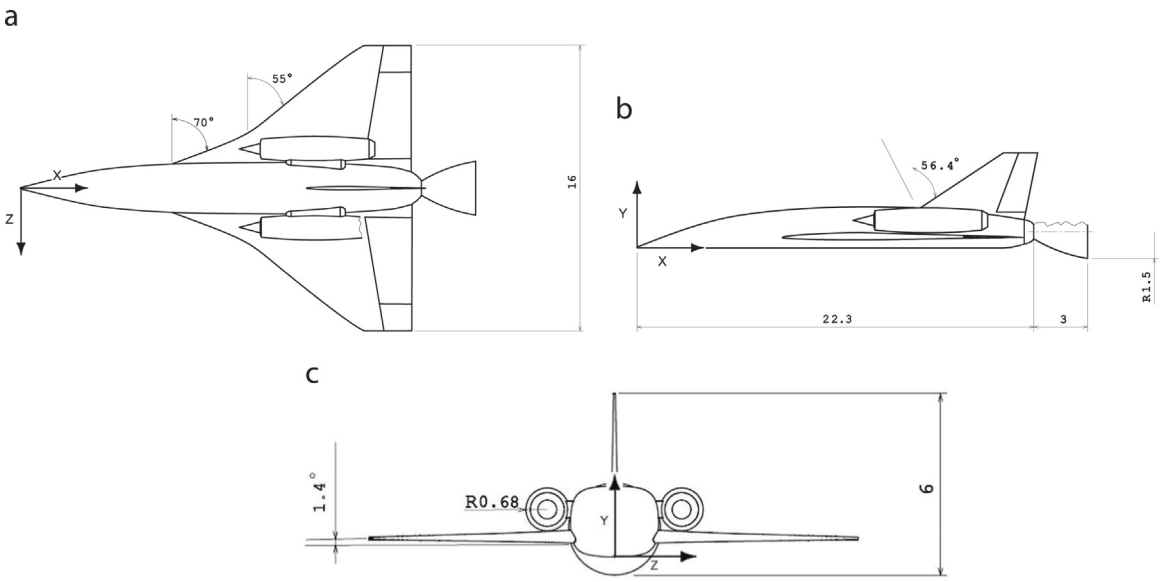

Fig. 2. (a) Top, (b) lateral and (c) front views of HyPlane; linear dimensions are in meters.

bottom to top and forms with the x-axis the meridian plane, the z (pitch) axis is along the wing span from right to left of the pilot and is perpendicular to the meridian plane. The center of mass (CoM) is located in the meridian plane ($z_{CoM}=0.0$ m) and moves back and forth of about one meter as the fuels is consumed. In the present study, the center of mass has been considered fixed at the abscissas $x_{CoM}=14.5$ m, $y_{CoM}=1.0$ m.

The wing plan form is a double wedge delta with an area $S_w=140$ m^2 and the wing span is $b=16$ m, therefore its aspect ratio ($\Lambda=b^2/S_w$) is about 1.83. The areas of each flap and of each aileron are 9.7 m^2 and 1.8 m^2 respectively, the area of the moving part of the rudder is 4.7 m^2. The reference area (S_{ref}) and length (L_{ref}), used for scaling the aerodynamic forces and moments to the related coefficients, are the wing plan form ($S_{ref}=S_w$) and the wing mean aerodynamic chord ($L_{ref}=10$ m).

3. Direct Simulation Monte Carlo method and DS3V code

It is well known that the Navier–Stokes equations fail in low density regimes, due to the failure of the "classical" laws of Newton, Fourier and Fick, computing the transport parameters. Even though nowadays the finite-difference solutions of the kinetic Boltzmann equation has been performed successfully, as evidenced by the high number of papers published on this topic (see paper by Chen and Doolen [13] and related references), however for the present application the Direct Simulation Monte Carlo (DSMC) method [14–16] has been preferred. In fact, DSMC is currently the most developed and the most widely used method for modeling complex super/hypersonic rarefied gas flows for the solution of rarefied flow fields from slip flow to free molecular regimes.

Philosophy of DSMC is different from the "traditional" fluid dynamics. In fact, the "traditional" fluid dynamics considers the gas like a continuous substance, modeled in terms of the physical parameters (density, pressure, temperature and so on). The solution of the flow field relies on the integration of differential equations. On the contrary, DMSC deals with the gas as made up of a number of discrete molecules with translational, rotational and vibrational energies. Movement of molecules and collisions with other molecules and with the body are governed by a number of analytical equations from the kinetic theory of gases. DSMC is not a numerical method, it has to be considered just like a computer method. The most important advantage is that it does not suffer from numerical instabilities and does not rely directly on similarity parameters like the Mach number, the Reynolds number. Shortcoming is that it is always unsteady; steady flow is achieved after a long enough simulated time and, therefore, it requires high processing velocity to reach steady conditions.

DSMC computes the evolution of millions of simulated particles, each one representing a large number (say 10^{15}) of real particles in the physical space. Intermolecular and molecule-surface collisions are taken into account. The computational domain is divided in cells which are used to select the colliding molecules and to sample the macroscopic fluid-dynamic quantities.

The present analysis relies on the DSMC code DS3V [12] for the computation of the HyPlane aerodynamic forces and moments. DS3V considers air as made up of five neutral reacting species (O_2, N_2, O, N and NO) and relies on the built-in Gupta–Yos–Thompson [17] chemical model, consisting of 23 reactions. The code can consider also surface reactions such as recombination reactions, therefore catalytic effects.

For the computation of normal and tangential stress on the surface, DS3V implements both the Maxwell and the Cercignani–Lampis–Lord (CLL) models [14–16], chosen optionally by the user. If the Maxwell model is selected, the user has to input the fraction (f) of molecules re-emitted diffusively: $f=1$ simulates a diffusive, fully accommodated re-emission, $f=0$ simulates a specular re-emission, intermediate values simulate an incomplete accommodation re-emission.

The code is "sophisticated" (termed also DSMC07). As widely reported in literature [18–21], a sophisticated code implements computing procedures providing efficiency and accuracy higher than those from a "basic" DSMC code (termed also DSMC94). A sophisticated code, in fact, is based on two sets of cells (collision and sampling cells) with the related cell adaptation and implements methods promoting nearest neighbor collisions. This type of code generates automatically computational parameters such as numbers of cells, of simulated particles by the input numbers of megabytes and of free stream number density and provides optimal time step. Finally, the same collision pair cannot have sequential collisions. This procedure avoids a second collision between the same collision partners; this is physically impossible because after a collision, the molecules move away in opposite directions.

Besides being "sophisticated", DS3V is also "advanced". It allows

Table 1
Input data to DS3V and overall Knudsen numbers.

h [km]	ρ_∞ [kg/m^3]	N_∞ [m^{-3}]	T_∞ [K]	$\alpha_{O_2\infty}$	$\alpha_{N_2\infty}$	$\alpha_{O\infty}$	$Kn_{\infty L}$
100	5.59×10^{-7}	1.19×10^{19}	196	0.1798	0.7750	0.0452	5.59×10^{-3}
90	3.39×10^{-6}	7.12×10^{19}	187	0.2075	0.7792	0.0133	9.37×10^{-4}
80	1.83×10^{-5}	3.84×10^{20}	199	0.2095	0.7808	0.0097	1.74×10^{-4}

the user to evaluate the quality of a simulation. The user can verify that the number of simulated particles and collision cells are adequate; this task is fulfilled by the on line visualization of the ratio between the molecule mean collision separation (mcs) and the mean free path (λ) in each computational cell. In addition, the codes allow the user to change, during a run, the number of simulated particles. The ratio mcs/λ has to be less than unity everywhere in the computational domain; more specifically, Bird [12,18–21] suggests 0.2 as a limit value for an optimal quality of the run. In addition, the code gives the user information about the stabilization of the runs by means of the profile of the number of simulated particles as a function of the simulated time. The stabilization of a DSMC calculation is achieved when this profile becomes jagged and included within a band defined by the standard deviation of the number of simulated particles.

4. Test conditions

Table 1 reports some free stream input data to DS3V and physical parameters at the altitudes (h) of 80, 90 and 100 km from the US Standard Atmosphere 1976. The free stream velocities, reported in Table 2, were such that, at the same altitudes, Mach numbers 2 and 3 are fulfilled. The Reynolds and the Knudsen numbers, based on the overall length of the vehicle (L=25.3 m) are also reported. The overall Knudsen numbers verify that the flow fields practically are in continuum low density regime or in slip flow. In fact, according to Moss [22], the transitional regime is defined by:

$10^{-3} < Kn_{\infty L} < 50$.

In this application, the diffusive, fully accommodated Maxwell model (f=1) has been used. The wall temperature (T_w=300 K) was supposed constant and uniform along the whole vehicle. Due to the low value of velocity therefore of the free stream energy level (H_∞) of the flow (see Table 2), dissociation of Oxygen and Nitrogen is negligible (the dissociation energy of Oxygen and Nitrogen are 15.4 and 33.6 MJ/kg, respectively) therefore no wall reaction was implemented.

Tests were carried out in the range of angles of attack (α) −5° to 30° with a step of 5°, considering HyPlane in clean configuration ($\delta=\vartheta=\gamma=0°$). Tests, evaluating the effectiveness of the HyPlane flaps, were carried out at h=100 km (M_∞=2), at zero angle of attack and in the range of the flaps deflection angle (δ) −25° to 25°. The computations in symmetric flight, i.e. with no aileron ($\vartheta=0°$) and with no rudder ($\gamma=0°$), took advantage of the symmetry of the flow field. Computations were, in fact, carried out on half body; the plane of symmetry of the vehicle lies on the x–y plane. The computing region was a parallelepiped: L_x=30 m, L_y =19 m and L_z=11 m. The computations in not-symmetric flight (i.e. with $\vartheta\neq0$ or $\gamma\neq0$) were carried out in a double sized parallelepiped L_x=30 m, L_y=19 m and L_z=22 m and at h=100 km and M_∞=2. Tests evaluating efficiency of the aileron (ϑ) and the rudder (γ) were carried out in the range of 0–25° at h=100 km. Also for these cases, the step of the deflection angle was 5°.

Table 2
Free stream velocity, dynamic pressure, total enthalpy, Mach and Reynolds numbers.

h [km]	V_∞ [m/s]	$p_{D\infty}$ [N/m^2]	H_∞ [MJ/kg]	M_∞	$Re_{\infty L}$
100	570	9.08×10^{-2}	3.59×10^{-1}	2	6.08×10^{2}
100	855	2.04×10^{-1}	5.63×10^{-1}	3	9.11×10^{2}
90	542	4.98×10^{-1}	3.35×10^{-1}	2	3.74×10^{2}
90	827	1.16×10^{-0}	5.30×10^{-1}	3	5.61×10^{2}
80	568	2.95×10^{-0}	3.61×10^{-1}	2	1.98×10^{4}
80	852	6.64×10^{-0}	5.63×10^{-1}	3	2.97×10^{4}

5. Accuracy of the computations

The input number of megabytes, used for the present tests, ranged in the interval 150–200. Unfortunately, the user can only roughly control the number of cells by setting the input number of divisions and elements in each division; the higher the number of elements the higher the number of the cells after the adaptation process. DS3V suggests an optimal number of molecules/cell for adapting both collision and sampling cells. An increment of the number of cells can be achieved also by inputting a smaller number of molecules/cell. All runs relied on a number of simulated molecules of about 5.5×10^6. As the cell adaptation process was fulfilled by means of 6 molecules for collision cell and 20 molecules for sampling cell, the number of collision and sampling cells were about 10^6 and 2.7×10^5. According to the logic of the DSMC adaptation process, the cells are not of the same size neither are uniformly distributed in the flow field. The cells are smaller and their number is higher where there is a higher number of molecules and thus where there is an higher density.

In addition to the mcs/λ parameter (as said before, a correct DSMC simulation is achieved when mcs/$\lambda<1$ everywhere in the computing dominion or in each collision cell), the quality of a DSMC run was evaluated also in terms of simulation time (t_s). In fact, the longer the simulation time the larger the sample size during a run and therefore the time averaging the fluid-dynamic quantities during the evolution toward the steady state conditions. The average of the molecular properties is equivalent to making the calculation with a larger number of molecules. It could then be possible to achieve a one to one correspondence between real and simulated molecules so that the fluctuations match those in real gas. A rule of thumb suggests to consider a run stabilized, from a fluid-dynamic point of view, when $t_s/t_f\cong10$; t_f is the time to travel the computing region at the free stream velocity. Finally, DS3V has a function to evaluate the stabilization of a run by means of the condition that the profile of the "molecule number history" gets jagged.

Even though the ratio mcs/λ is a local parameter, computed in each collision cell, Table 3 reports values of mcs/λ, averaged in the flow field, obtainable by the 2-D plot shown during the DS3V run. Table 3 reports also the ratio t_s/t_f. To be conservative both mcs/λ and t_s/t_f reported in the table are those obtained at the most severe test conditions:

- α=30° in clean configuration.
- α=0° with the control surfaces deflected at maximum angles:

$\delta=-25°$, $\delta=25°$, $\vartheta=\pm 25°$ and $\gamma=25°$.

It is shown that all computations at $h=100$ km satisfy the requirements of accurate computations from both DSMC and aerodynamic points of view. Even though the values of mcs/λ do not satisfy the optimal limit value of 0.2 by Bird, they are always smaller than one in each run, as required by the method.

As reported in Table 4, the same remark about the ratio mcs/λ can be made for the tests at $h=90$ km. On the contrary, at $h=80$ km the DSMC calculation accuracy requirements is not satisfied and, by the way, DS3V runs are more demanding. This is coherent with the intrinsic DSMC formulation as reported by Bird [15], because the duration of the physical flow time increases with decreasing rarefaction. Thus, considering that, at around 80 km altitude, the rarefaction level makes problematic the solution of a flow field by both DSMC and Navier–Stokes solvers as well, the results obtained in the present work can be accepted as preliminary and only qualitatively indicative of the aerodynamic behavior of HyPlane. On the other hand, an improvement of the DSMC results in terms of reducing mcs/λ is technically feasible by using a larger number of simulated molecules and collision cells, implying more powerful computer both in terms of core storage and processing velocity. The current trend is using versions of DSMC code operating on multi-processors computers.

Table 3
Quality of computation at $h=100$ km.

	$\alpha=30°$	$\delta=-25°$	$\delta=25°$	$\vartheta=\pm 25°$	$\gamma=25°$
mcs/λ	0.7	0.6	0.6	0.4	0.5
t_s/t_f	12	9	19	59	106

Table 4
Quality of computation at $h=90$ and $h=80$ km.

	$h=90$ km, $\alpha=30°$	$h=80$ km, $\alpha=30°$
mcs/λ	0.9	2
t_s/t_f	6	9

6. Analysis of results

Fig. 3(a) and (b) show the 3-D maps of the pressure distribution on the top (a) and on the bottom (b) surface of HyPlane at $h=100$ km, $\alpha=20°$, $\delta=25°$, $\vartheta=\pm 10°$ and $\gamma=0°$. Due to the low values of both free stream velocity and density, the total pressure is very low; the full scale of the graphics is about 8×10^{-2} Pa, free stream static pressure at $h=100$ km is 3.22×10^{-2} Pa and pressure on the lower surface is about 4 times that on the upper surface.

Fig. 4(a)–(d) show the profiles of the lift (C_L (a)) and drag (C_D (b)) coefficients, aerodynamic efficiency (C_L/C_D (c)) and pitching moment coefficient (C_{MZ} (d)); the reduction pole is the center of mass. The computations were carried out in clean configuration ($\delta=\vartheta=\gamma=0°$) as functions of the angle of attack (α) at $h=80$, 90 and 100 km and at the free stream Mach numbers 2 and 3 with no thrust by both the engines and the rocket.

In agreement with the well known supersonic similarity rule ($C_p = C_{pi}/\sqrt{M_\infty^2-1}$ where C_p is the pressure coefficient and "i" is for incompressible flow [23]), the lift, drag and moment coefficients at $M_\infty=3$ are smaller than those at $M_\infty=2$, being these aerodynamic coefficients integrals of the pressure coefficients along the body surface.

Tables 5 and 6 make possible the quantification of the effects of the Mach, Reynolds and Knudsen numbers by means of important aerodynamic parameters such as the slopes of the lift and of the pitching moment coefficients versus the angle of attack, the minimum drag coefficient and the maximum aerodynamic efficiency. Being the lift and moment curves pretty linear, the slopes ($dC_L/d\alpha$ and $dC_{Mz}/d\alpha$) have been computed on the whole interval of angles of attack by the ratios of finite differences $\Delta C_L/\Delta\alpha$ and $\Delta C_{Mz}/\Delta\alpha$.

The lift curve slope decreases with both the free stream Mach and Knudsen numbers while the influence of both numbers on the pitching moment coefficient slope appears to be secondary. The minimum drag coefficient is influenced both by the Knudsen and the Reynolds numbers; it increases with the Knudsen number and decreases with the Reynolds number. The minimum drag coefficients are met at $\alpha=0°$ at all analyzed conditions. The maximum efficiency is influenced in opposite direction of the drag coefficient by the Knudsen and Reynolds numbers. The angle of maximum efficiency is 20° at all analyzed conditions.

Fig. 4(d) verifies that, at each altitude and Mach number, the longitudinal equilibrium ($C_{Mz}=0$) is achieved at an angle of attack of $\alpha\cong-5°$. A positive flap deflection (i.e. anti-clock-wise or

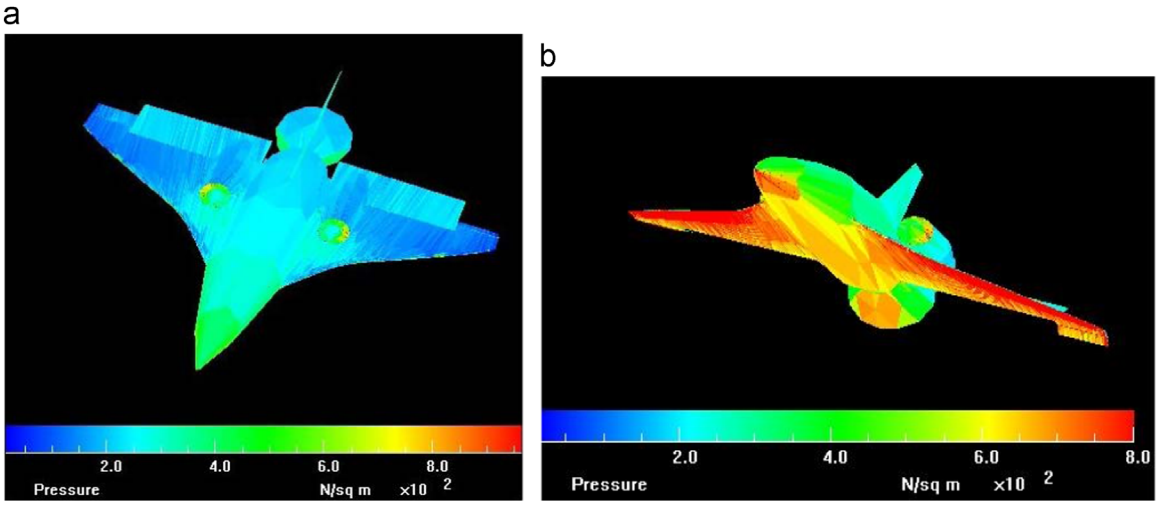

Fig. 3. 3-D maps of pressure on the top (a) and on the bottom surface of HyPlane: $h=100$ km, $\alpha=20°$, $\delta=25°$, $\vartheta=\pm 10°$, and $\gamma=0°$.

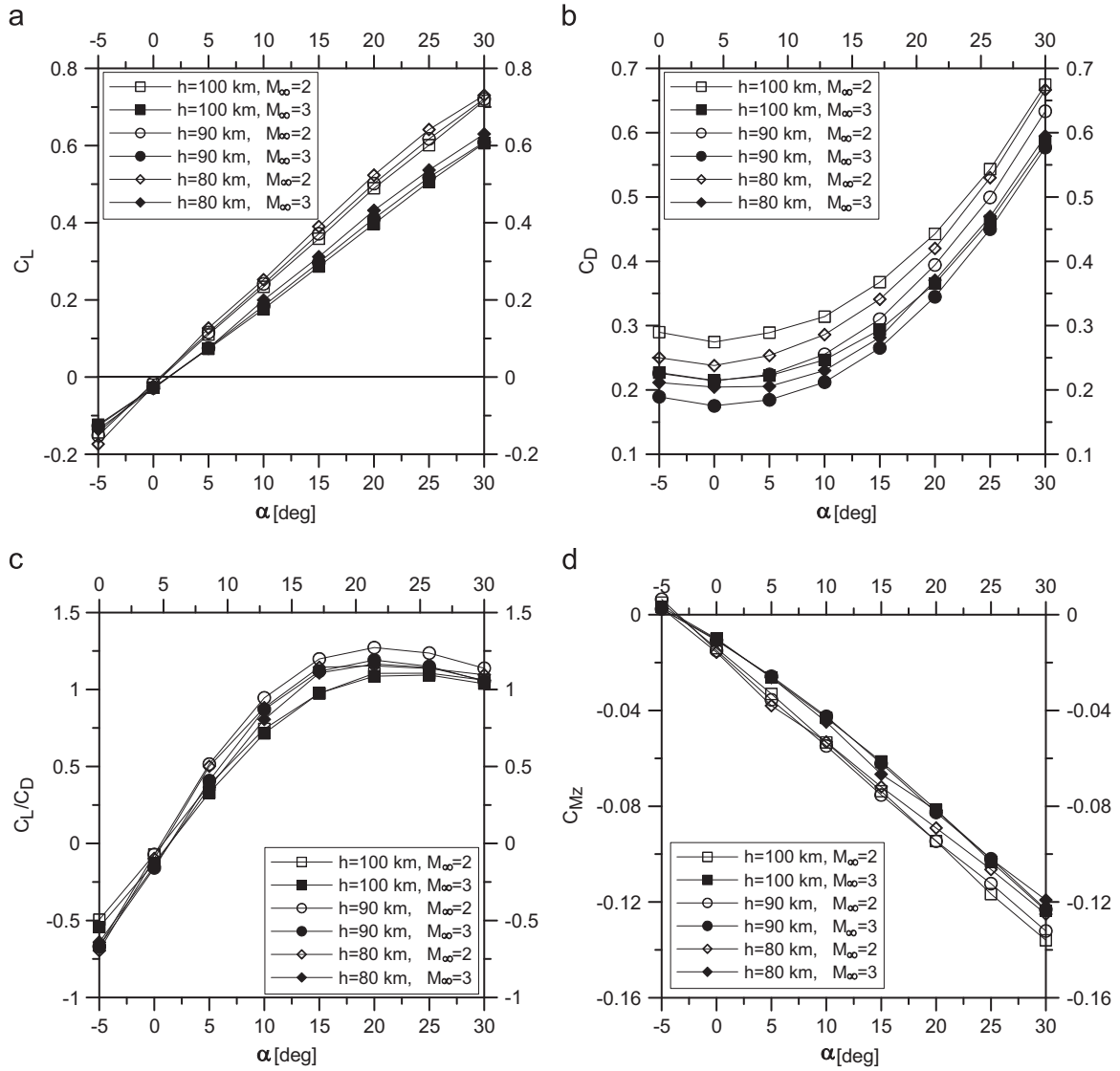

Fig. 4. (a) Lift coefficient, (b) drag coefficient, (c) aerodynamic efficiency and (d) pitching moment coefficient in clean configuration as function of the angle of attack.

Table 5
Aerodynamic parameters at $M_\infty=2$.

h [km]	$\Delta C_L/\Delta\alpha$ [deg.$^{-1}$]	$\Delta C_{Mz}/\Delta\alpha$ [deg.$^{-1}$]	C_{Dmin}	$(C_L/C_D)_{max}$
100	0.0246	−0.0040	0.2745	1.1060
90	0.0249	−0.0040	0.2142	1.2719
80	0.0258	−0.0037	0.2378	1.1442

Table 6
Aerodynamic parameters at $M_\infty=3$.

h [km]	$\Delta C_L/\Delta\alpha$ [deg.$^{-1}$]	$\Delta C_{Mz}/\Delta\alpha$ [deg.$^{-1}$]	C_{Dmin}	$(C_L/C_D)_{max}$
100	0.0208	−0.0036	0.2147	1.0933
90	0.0210	−0.0036	0.1752	1.1912
80	0.0219	−0.0035	0.2044	1.1659

upward) of $\delta=25°$ involves a shift of the equilibrium angle of attack to about 5°. As shown in Fig. 5, this deflection of the flap produces a different aerodynamic behavior of the vehicle. More specifically, at $h=100$ km and $M_\infty=2$, the effects of a flap deflection of $\delta=25°$ are:

i. The zero lift angle of attack moves from 0 to 5°.
ii. C_{Dmin} (at $\alpha=0°$) increases from 0.2745 to 0.2851, the percentage variation is about 4%.
iii. $\Delta C_L/\Delta\alpha$ decreases from 0.0246 to 0.0240 [deg.$^{-1}$], the percentage variation is −2%.
iv. $(C_L/C_D)_{max}$ decreases from 1.1060 to 1.054, the percentage variation is −4%.
v. $\Delta C_{Mz}/\Delta\alpha$ increases from −0.0040 to −0.0035 [deg.$^{-1}$], the percentage variation is −13%.

As reported in Fig. 5(d), the displacement of the center of mass strongly reduces the pitching moment slopes. For example, if $x_{CoM}=15.0$ m is assumed as reduction pole, the values of $\Delta C_{Mz}/\Delta\alpha$ are −0.0013 and −0.0001 [deg.$^{-1}$] in clean and flapped configuration, respectively. If $x_{CoM}=14.5$ m is assumed as reduction pole, these values are −0.0041 and −0.0034, respectively.

In order to enhance the aerodynamic analysis of HyPlane, in rarefied flow, its global aerodynamic coefficients, are compared with those of SpaceLiner computed by Zuppardi et al. [9] by means of the same DSMC code. Considering the different aerodynamic test conditions or Knudsen, Mach and Reynolds numbers ($Kn_{L\infty}=2.16\times10^{-3}$, $Ma_\infty=12$ and $Re_{L\infty}=8.04\times10^3$ for SpaceLiner) and ($Kn_{L\infty}=5.59\times10^{-3}$, $Ma_\infty=3$ and $Re_{L\infty}=9.11\times10^2$ for

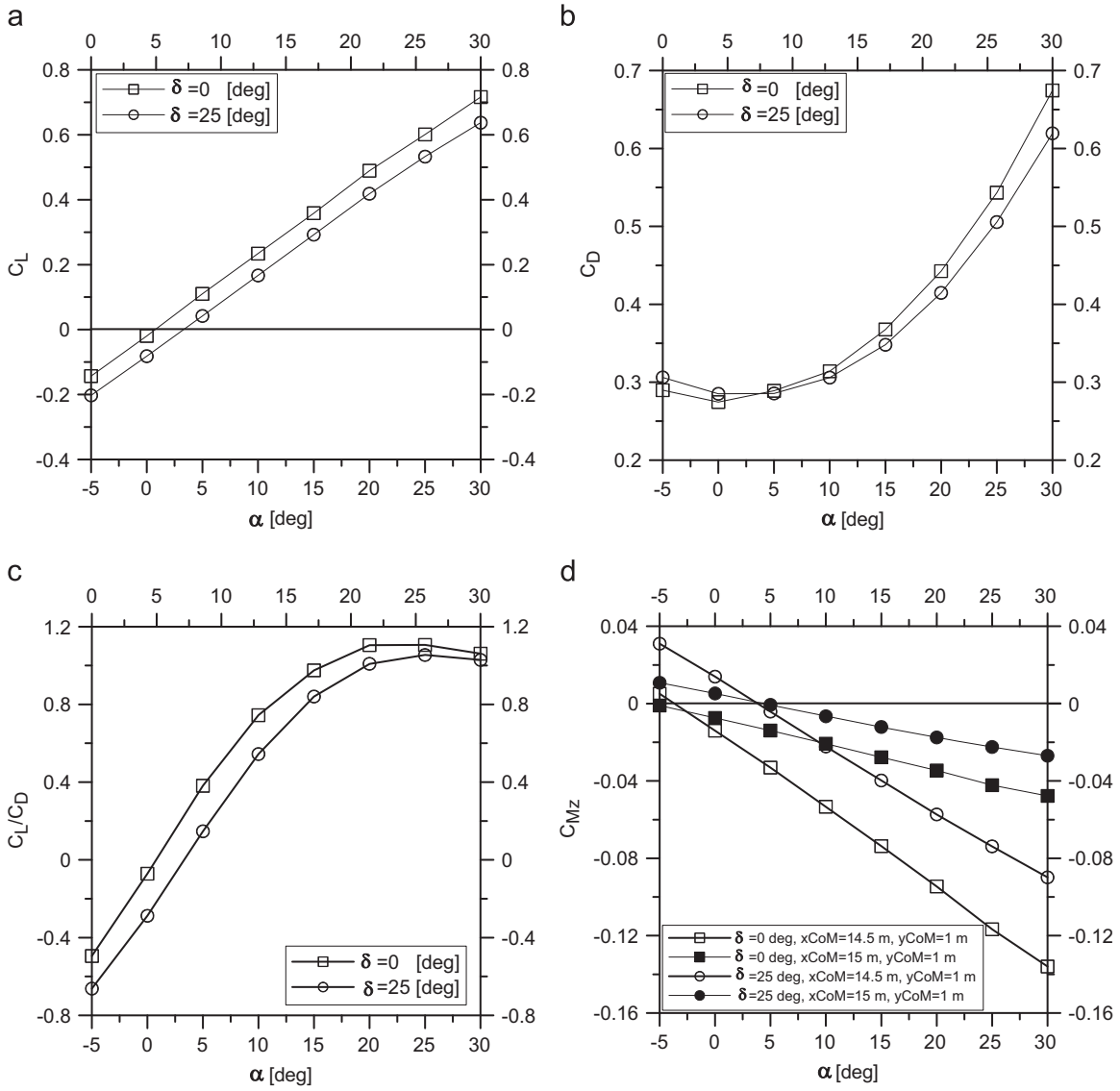

Fig. 5. Comparison of (a) lift coefficient, (b) drag coefficient, (c) aerodynamic efficiency and (d) pitching moment coefficient in clean configuration and in configuration with a flap deflection of $\delta=25°$ as function of the angle of attack: $h=100$ km, $M_\infty=2$.

HyPlane) linked to the different dimensions of the airplanes (the fuselage length of SpaceLiner is 63 m) and to the different free stream velocity (the free stream velocity of SpaceLiner is 4500 m/s) linked to different trajectories, the comparison can provide only preliminary information. Fig. 6(a), (b), (c) and (d), compare the lift, drag, aerodynamic efficiency and longitudinal moment coefficients and Table 7 reports the values of some meaningful parameters evaluated at $h=100$ km. The values reported in the table indicate that the aerodynamic behavior, at this altitude, of SpaceLiner is better than that of HyPlane.

Trim conditions are calculated considering for each angle of attack the flaps deflection necessary in order to bring the aerodynamic center near to the center of mass. Tables 8 and 9 show the trim angles of attack for the flight conditions of $h=100$ km, $M_\infty=2$ and $h=80$ km, $M_\infty=3$, respectively. The trim angle is always in the range $-5°$ to $5°$. The equilibrium attitude at small angle of attack could be therefore guaranteed with continuous variation of the flaps deflection during the suborbital parabola. For higher angles of attack, the flaps deflections should become too large to be realistic. The lift, drag coefficients and the related aerodynamic efficiency are reported to evaluate the coupling effects of the flap deflection and the trim angles, in particular a flap deflection of 25° and the trim angle of $+5°$ makes the lift positive.

In order to provide the flight mechanic designer with direct and immediate information about the HyPlane attitude control capability on the longitudinal and lateral-directional planes by means of aerodynamic surfaces, the aerodynamic moments are plotted in terms of dimensional quantities. The moments, shown in the following figures, are those computed at $\alpha=0°$, $h=100$ km and $M_\infty=2$ conditions (Table 2). Fig. 7(a) shows the effects of the flaps deflection (δ) on the pitching moment (M_z). Fig. 7(b) and (c) provide an evaluation of the effects of the deflection angles of the ailerons (ϑ) and of the rudder (γ) on the rolling (M_x) and yawing (M_y) moments. Also the rolling and the yawing moments are computed around the center of mass located at $x_{CoM}=14.5$ m. In order to quantify the effects of the aerodynamic control surfaces, Table 10 reports the slopes averaged on all deflection angles. The effects of the ailerons are prevalent on the rolling and the effects of the rudder are prevalent on the yawing moments. In fact, the effect on the rolling moment produced by the ailerons

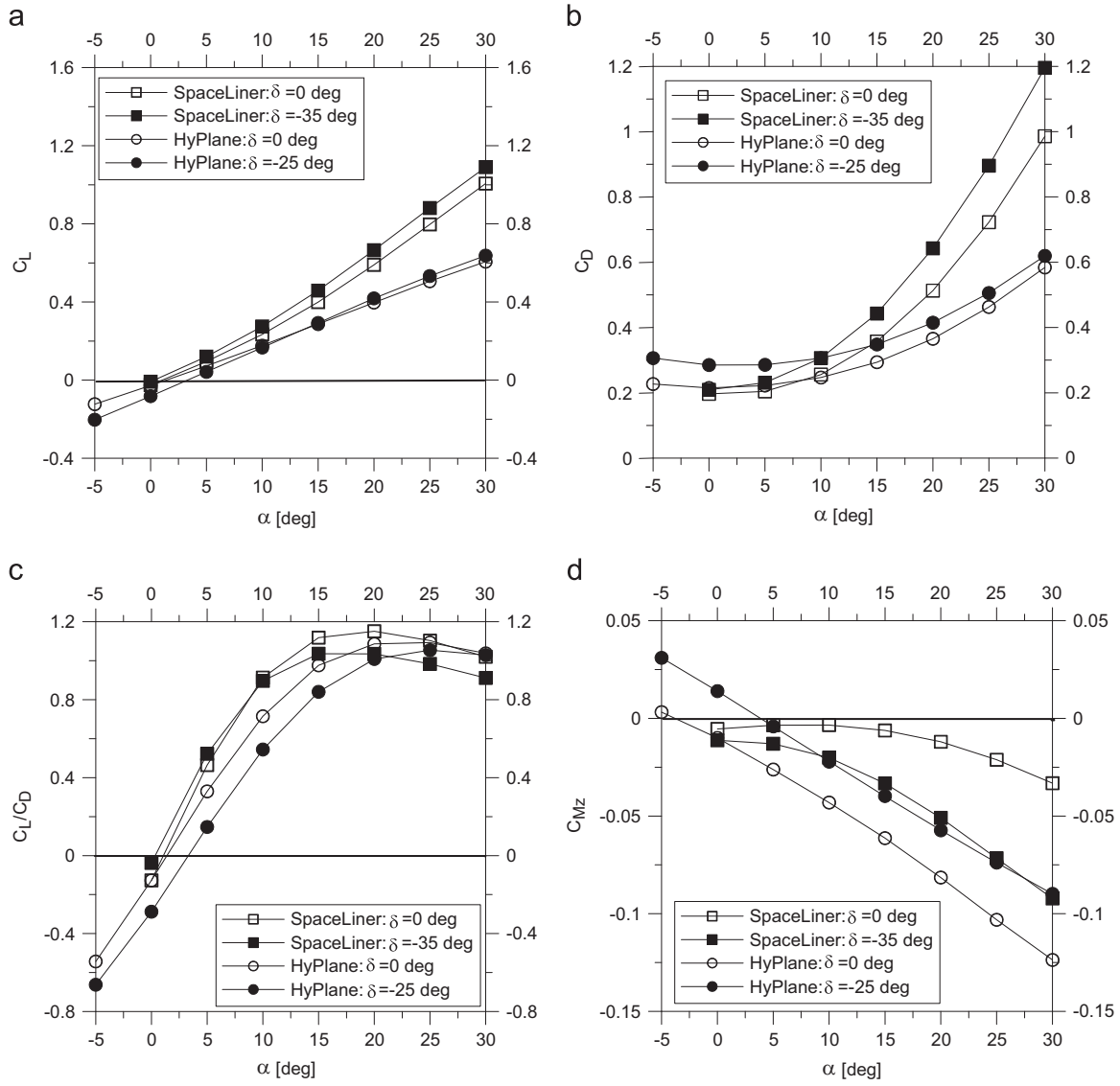

Fig. 6. Comparison of (a) lift coefficient, (b) drag coefficient, (c) aerodynamic efficiency and (d) pitching moment coefficient in clean and flapped configurations of the SpaceLiner and HyPlane vehicles as function of the angle of attack: $h=100$ km.

Table 7
Comparison of aerodynamic parameters at $h=100$ km.

Vehicle	$\Delta C_L/\Delta\alpha$ [deg.$^{-1}$]	$\Delta C_{Mz}/\Delta\alpha$ [deg.$^{-1}$]	C_{Dmin}	$(C_L/C_D)_{max}$
SpaceLiner, $\delta=0°$	0.0344	−0.0009	0.1968	1.1509
SpaceLiner, $\delta=-35°$	0.0366	−0.0027	0.2091	1.0356
HyPlane, $\delta=0°$	0.0208	−0.0036	0.2147	1.0933
HyPlane, $\delta=-25°$	0.0240	−0.0035	0.2851	1.0542

Table 8
Equilibrium angles of attack and corresponding. aerodynamic parameters: $h=100$ km, $M_\infty=2$.

δ [deg.]	α_{trim} [deg.]	C_L	C_D	C_L/C_D
0	−5	−0.0585	0.1183	−0.4947
15	0	−0.0238	0.1200	−0.1983
25	5	0.0171	0.1166	0.1469

deflection is about four times larger than that produced by the rudder deflection while the effect on the yawing moment by the rudder is about twice larger than that due to the ailerons.

Table 9
Equilibrium angle of attack and corresponding.aerodynamic parameters: $h=80$ km, $M_\infty=3$.

δ [deg.]	α_{trim} [deg.]	C_L	C_D	C_L/C_D
0	−5	−0.0553	0.0863	−0.6407
15	0	−0.0230	0.0807	−0.2854
25	5	0.0377	0.2207	0.1708

By neglecting the effects of the Knudsen, Reynolds and Mach numbers, a preliminary evaluation of the aerodynamic moments at other flight conditions in the altitude interval 80–100 km and in the Mach number interval 2–3, can be preliminary achieved by scaling these data via the free stream dynamic pressure ($p_{D\infty}$, see Table 2).

7. Conclusions

Since preliminary computations verified that the propulsion system of the Italian space tourism vehicle HyPlane allows this aerospaceplane to reach altitudes as high as 100 km and more, in

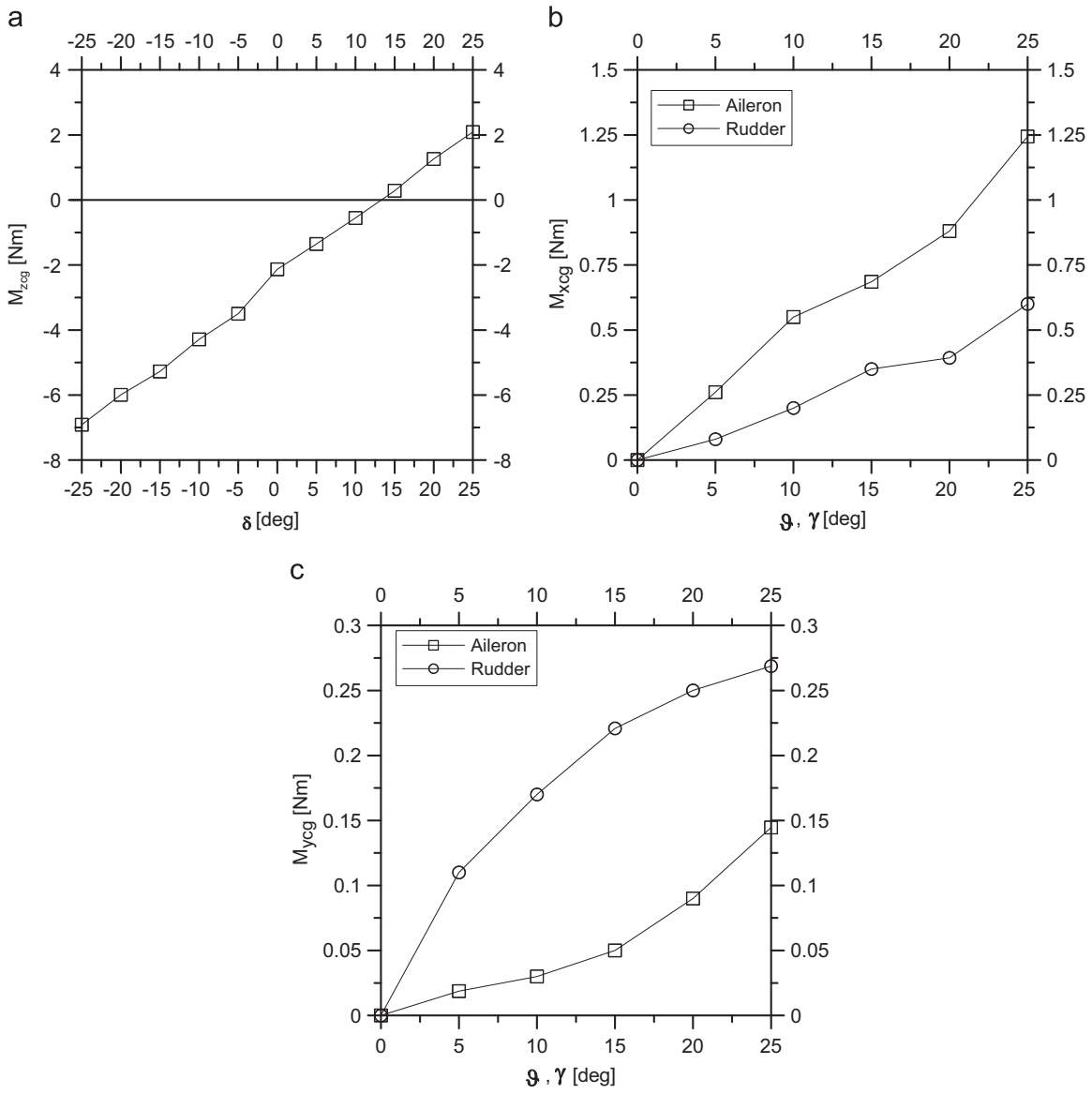

Fig. 7. Influence of the deflection angle of the flaps on the pitching moment (a) and of ailerons and rudder on the rolling (b) and yawing (c) moments.

Table 10
Slopes of moments versus the deflection angle of the control surfaces.

$dM_z/d\delta$ [Nm/deg.]	$dM_x/d\vartheta$ [Nm/deg.]	$dM_x/d\gamma$ [Nm/deg.]	$dM_y/d\vartheta$ [Nm/deg.]	$dM_y/d\gamma$ [Nm/deg.]
0.1800	0.0493	0.0206	0.0041	0.0154

the present paper some aspects of the aerodynamic behavior of the vehicle have been analyzed in rarefied (continuum low density) regime. Computations by the DSMC code DS3V have been carried out at the altitudes of 80, 90 and 100 km and at Mach number of 2 and 3. The aerodynamic behavior, in terms of global coefficients, has been compared also with that of SpaceLiner at 100 km both in clean and flapped configuration.

Computations showed that, in clean configuration and at high altitude, the trim angle of attack is about $-5°$ and that thanks to the flap deflection of $+25°$ the trim angle of attack shifts to 5°, verifying the longitudinal attitude control capability. Other attitude control capabilities related to ailerons and rudder have been also evaluated. Tests have been carried out at zero angle of attack and 100 km altitude, in the $-25°$ to 25° flaps deflection angle range and in the 0–25° ailerons and rudder deflection angle range. An evaluation of the aerodynamic moments at other analyzed test conditions can be preliminary fulfilled by scaling these data with the dynamic pressure.

The verified HyPlane attitude control capability by means of aerodynamic surfaces is very useful because allows HyPlane to reduce the amount of fuel for the thrusters.

References

[1] V. Carandente, V. D'Oriano, A. Gallina, G. Russo, R. Savino, Aerothermodynamic and system analysis of a small hypersonic airplane (HyPlane), in: Proceedings of the 64th International Astronautical Congress, Beijing, China, 2013.
[2] R. Savino, G. Russo, V. D'Oriano, M. Visone, M. Battipede, P. Gili. Performances of a small hypersonic airplane (HyPplane), in: Proceedings of the 65th International Astronautical Congress, Toronto, Canada, Acta Astronautica, 2014, 115, 2015, pp. 338–348.
[3] R. Savino, G. Russo, V. Carandente, V. D'Oriano, HyPlane: challenges for space tourism and business transportation, J. Aeronaut. Aerosp. Eng. 2 (2013) 1–8.
[4] R. Savino, G. Russo, V. Carandente, V. D'Oriano, HyPlane for space tourism and business transportation, JBIS 67 (2014) 82–89.
[5] G. Russo, PRORA-USV: Closer Space and Aeronautics, West-East High Speed

Flow Field (WEHSFF-2007) Conference, Moscow, Russia, 2007.
[6] ⟨https://it.wikipedia.org/wiki/Space_Shuttle⟩.
[7] M. Sippel, A. van Foreest, C. Bauer, F. Cremaschi, System Investigation of the SpaceLiner Concept in FAST20XX, 2011, AIAA Paper, pp. 2011–2294.
[8] M. Sippel et al., Technical maturation of the spaceliner concept, in: Proceedings of the 18th AIAA/3AF International Space Planes and Hypersonic Systems and Technologies Conference, Tours, France, 2012.
[9] G. Zuppardi, L. Morsa, M. Sippel, T. Schwanekamp, Aero-thermo-dynamic analysis of the spaceLiner-7.1 vehicle in high altitude flight, in: Proceedings of the 29th International Symposium on Rarefied Gas Dynamics, Xi'an, China, 2014.
[10] ⟨https://en.wikipedia.org/wiki/SpaceShipTwo⟩.
[11] ⟨https://it.wikipedia.org/wiki/Concorde⟩.
[12] G.A. Bird, The DS3V Program User's Guide Ver. 2.5, G.A.B. Consulting Pty. Ltd. Sydney, Australia, 2006.
[13] S. Chen, G.D. Doolen, Lattice Boltzmann method for fluid flows, Annu. Rev. Fluid Mech. 30 (1998) 329–364.
[14] G.A. Bird, Molecular Gas Dynamics and Direct Simulation Monte Carlo, Clarendon Press, Oxford, Great Britain, 1998.
[15] G.A. Bird, The DSMC Method, Version 1.1, Amazon, ISBS 9781492112907, Charleston, USA, 2013.
[16] C. Shen, Rarefied Gas Dynamic: Fundamentals, Simulations and Micro Flows, Springer-Verlag, Berlin, Germany, 2005.
[17] R.N. Gupta, J.M. Yos, R.A. Thompson, A Review of Reaction Rates and Thermodynamic Transport Properties for an 11-Species Air Model for Chemical and Thermal Non-Equilibrium Calculations to 30,000 K, NASA TM 101528, 1989.
[18] G.A. Bird, Sophisticated versus simple DSMC, in: Proceedings of the 25th International Symposium on Rarefied Gas Dynamics, Saint Petersburg, Russia, 2006.
[19] G.A. Bird, M.A. Gallis, J.R. Torczynski, D.J. Rader, Accuracy and efficiency of the sophisticated Direct Simulation Monte Carlo algorithm for simulating non-continuum gas flows, Phys. Fluids 21 (2009) 017103.
[20] M.A. Gallis, J.R. Torczynski, D.J. Rader, G.A. Bird, Convergence behavior of a new DSMC algorithm, J. Comput. Phys. 228 (2009) 4532–4548.
[21] G.A. Bird, The DS2V/3V program suite for dsmc calculations, in: Proceedings of the 24th International Symposium on Rarafied Gas Dynamics Monopoli, Italy, 2004.
[22] J.N. Moss, Rarefied Flows of Planetary Entry Capsules, Special course on Capsule Aerothermodynamics, Rhode-St.-Genèse, Belgium, AGARD-R 808, 1995, pp. 95–129.
[23] A. Shapiro, The Dynamics and Thermodynamics of Compressible Fluid Flow, John Wiley & Sons Inc, New York, USA, 1953.

Gennaro Zuppardi got a Laurea degree in Aeronautical Engineering in July 1976 (score: 110/110) at the University of Naples "Federico II". He has been a lecturer in: 1) Fluid-dynamics at the University of Basilicata (a.y. 1993/94), 2) Experimental Fluid-dynamics at the University of Naples "Federico II" (a.y. 1994/95), 3) Hypersonic Aerodynamics at the University of Naples "Federico II", since a.y. 1997/98 up today. Research activities: 1) Boundary layer diagnostics by non-intrusive technique (thermography), 2) Adaptive walls wind tunnel. 3) Aero-thermo-chemistry. 4) Rarefied Gas-Dynamics and DSMC, this subject is his current mayor. He is author or co-author of 90 scientific papers and of a book in Hypersonic Aerodynamics.

Raffaele Savino, Ph.D., is professor of Aerodynamics at the University of Naples Federico II. He was responsible as of several research programs in collaboration with Research Centers and Space Agencies (ASI, CIRA, ESA, NASA). His memberships include the International Academy of Astronautics (IAA), the International Astronautical Federation (IAF), the Italian Association of Aeronautics and Astronautics (AIDAA), the American Institute of Aeronautics and Astronautics (AIAA). He is author of over 200 publications in the fields of Fluid Dynamics, Microgravity and Space Experimentation, Physics of Fluids, Hypersonic Aerodynamics, Heat transfer, Aerospace Propulsion Recent research activities include hypersonic numerical and experimental aerodynamics, aerothermochemistry, innovative heat pipes for ground and space applications, hybrid rocket propulsion.

Gennaro Russo, Co-founder and President of TRANSTECH, an SME devoted to technology transfer and high tech projects. Co-conceiver and project manager of the HyPlane project. For 25 years he managed space related programs, projects and facilities devoted to space transportation and reentry at the Italian Aerospace Research Center. He was designer of the 70 MW SCIROCCO Plasma Wind Tunnel for reentry aerothermodynamics simulation. At the beginning of his career, he worked for about ten years with the Microgravity Research Team of University of Naples, designing, preparing and analyzing some experiments executed on board the ESA Spacelab. He is vice-president of the Italian Institute for the Future and DG of its Center for Near Space devoted to Space Tourism.

Luca Spano' Cuomo is a student in Aerospace Engineering at the University of Naples "Federico II". He is currently involved in the study of Aerodynamics of aero-space-planes in rarefied flow by means of Direct Simulation Monte Carlo codes. More specifically, during his Laurea Thesis, he developed several Rhinoceros CADs of HyPlane for running the DSMC code DS3V.

Eliano Petrosino got a Master degree in Aerospace Engineering In July 2015 (score 104/110) at the University of Naples "Federico II". The title of the thesis was "Influence of gas-surface interaction models on the aerodynamic parameters of an airfoil in hypersonic, rarefied flow". He has been collaborating with the research group of the projects "HyPlane" and "MISTRAL" at the University of Naples "Federico II". Since October 2015 he has been working at CGM Italia s.r.l. as technical office manager.